Published online 19 December 2022 *Nucleic Acids Research, 2022, Vol. 50, No. 22* **12969–12978**
https://doi.org/10.1093/nar/gkac1156

A subclass of archaeal U8-tRNA sulfurases requires a [4Fe–4S] cluster for catalysis

Nisha He[1,†], Jingjing Zhou[1,†], Ornella Bimai[1], Jonathan Oltmanns[2], Jean-Luc Ravanat[3], Christophe Velours[4,5], Volker Schünemann[2], Marc Fontecave[1] and Béatrice Golinelli-Pimpaneau[1,*]

[1]Laboratoire de Chimie des Processus Biologiques, Collège de France, CNRS, Sorbonne Université, 11 Place Marcelin Berthelot, 75231 Paris cedex 05, France, [2]Technische Universität Kaiserslautern, Fachbereich Physik, Erwin-Schrödinger-Str. 46, D-67663 Kaiserslautern, Germany, [3]University of Grenoble Alpes, CEA, CNRS, IRIG, SyMMES UMR 5819, F-38000 Grenoble, France, [4]Institute for Integrative Biology of the Cell (I2BC), CEA, CNRS, Université Paris-Saclay, Avenue de la Terrasse, 91198 Gif-sur-Yvette cedex, France and [5]Present address: Fundamental Microbiology and Pathogenicity Lab (MFP), UMR 5234 CNRS-University of Bordeaux, SFR TransBioMed. Bordeaux, France

Received May 18, 2022; Revised October 22, 2022; Editorial Decision November 14, 2022; Accepted November 21, 2022

ABSTRACT

Sulfuration of uridine 8, in bacterial and archaeal tRNAs, is catalyzed by enzymes formerly known as ThiI, but renamed here TtuI. Two different classes of TtuI proteins, which possess a PP-loop-containing pyrophosphatase domain that includes a conserved cysteine important for catalysis, have been identified. The first class, as exemplified by the prototypic *Escherichia coli* enzyme, possesses an additional C-terminal rhodanese domain harboring a second cysteine, which serves to form a catalytic persulfide. Among the second class of TtuI proteins that do not possess the rhodanese domain, some archaeal proteins display a conserved CXXC + C motif. We report here spectroscopic and enzymatic studies showing that TtuI from *Methanococcus maripaludis* and *Pyrococcus furiosus* can assemble a [4Fe–4S] cluster that is essential for tRNA sulfuration activity. Moreover, structural modeling studies, together with previously reported mutagenesis experiments of *M. maripaludis* TtuI, indicate that the [4Fe–4S] cluster is coordinated by the three cysteines of the CXXC + C motif. Altogether, our results raise a novel mechanism for U8-tRNA sulfuration, in which the cluster is proposed to catalyze the transfer of sulfur atoms to the activated tRNA substrate.

INTRODUCTION

s^4U is found at position 8 in the loop region connecting the acceptor stem and the D-stem of bacterial and archaeal tRNAs (1,2). s^4U is a sensor for near-UV exposure and it mediates cellular responses to UV stress (3,4). The ThiI name was given to the enzyme catalyzing sulfuration (thiolation) of U8-tRNA because the corresponding gene was initially identified as being involved in thiamin biosynthesis in *Escherichia coli* (5). It is now recognized that U8-tRNA sulfurases should not be called ThiI proteins (6) because most *thiI* genes play no role in the thiamine pathway (7,8). Indeed, only the rhodanese-like domain (RHD) of ThiI is required for sulfuration in the synthesis of thiamine (9) and this domain is rarely present in enzymes that catalyze the biosynthesis of s^4U8-tRNA (Supplementary Figure S1). To avoid confusion, we rename here this enzyme TtuI for **t**RNA **t**hio**u**ridine I.

Most eukaryotes lack TtuI proteins, as exemplified by the fact that the gene was found in only two protists out of 60 eukaryotic organisms tested (2). Interestingly, s^4U has also been found at position 9, in addition to position 8, in some archaeal tRNAs, such as *Thermoplasma acidophilum* (10). It is likely that a multi-site specific TtuI protein is involved in sulfuration at both positions 8 and 9 when these two neighboring positions are modified in tRNAs.

Two main classes of TtuI proteins have been identified. TtuI from γ-proteobacteria and from archaea of the genus *Thermoplasma* possess a C-terminal RHD (11,12), whereas other TtuI proteins do not possess this RHD extension (2) (Supplementary Figure S1). Yet, all TtuI enzymes contain a characteristic N-terminal ferredoxin-like domain (NFLD), present in functionally diverse groups of evolutionnarily-

*To whom correspondence should be addressed. Tel: +33 1 44 27 12 52; Fax: +33 1 44 27 14 83; Email: beatrice.golinelli@college-de-france.fr
†The authors wish it to be known that, in their opinion, the first two authors should be regarded as Joint First Authors.

related proteins, followed by a so-called THUMP domain and a PP-loop-containing pyrophosphatase domain (catalytic domain). The THUMP domain is known to specifically interact with tRNAs that are modified at position 6, 8 or 10, since it is found in tRNA-guanine(6)-N2 methyltransferase (13), tRNA-guanine(10)-N2,N2 methyltransferase (14) and tRNA-cytidine(8) deaminase (15). The PP-loop motif of TtuI enzymes binds ATP, which allows the formation of an adenylated tRNA intermediate (Supplementary Figure S2A) (16).

In the case of *E. coli* TtuI (EcTtuI), it has been shown that Cys456 from the RHD can accept sulfur as a persulfide from the cysteine desulfurase IscS (11) and that a second cysteine, Cys344 belonging to the catalytic domain, is involved in the reaction (17). Two possible mechanisms, involving these two cysteines as catalytic residues, have been proposed. In both cases, the first step consists in the activation of C4 of U8 by adenylation using ATP (Supplementary Figure S2A). Then, in the first scenario (Supplementary Figure S2B), a persulfide, formed on Cys456 of the RHD, directly attacks the activated uridine residue, releasing AMP. Next, Cys344 attacks and cleaves the disulfide bond linking the enzyme to the tRNA, leaving a thiouridine on the tRNA and a disulfide bond between Cys344 and Cys456 (17). In the second scenario (Supplementary Figure S2C), Cys344 attacks the persulfide group on Cy456 to form a disulfide bond, thus releasing a hydrogenosulfide. The latter is a nucleophile that can attack the activated uridine, releasing AMP and thiouridine. In both mechanisms, the protein ends up with a Cys456–Cys344 disulfide bond and recycling the catalytic cysteines for the next catalytic cycle requests the reduction of that disulfide bond. This step would explain why TtuI cannot achieve more than one turnover in the absence of reductants (17,18). In *in vitro* activity assays, catalytic turnover is achieved thanks to dithiothreitol (DTT), as the reductant.

Several enzymes that do not possess the RHD extension have been studied biochemically or structurally (7,19–21). In particular, the crystal structure of *Bacillus anthrasis* TtuI (BaTtuI) has been solved in complex with AMP (19) and that of *Thermotoga maritima* (TmTtuI) in complex with a mini-RNA, in the presence or absence of ATP (20). These enzymes lack the RHD but possess a cysteine in the catalytic domain, at a position equivalent to Cys344 in *E. coli* (Supplementary Figure S1). This cysteine in TmTtuI (numbered Cys344) has been shown to be important for catalytic activity (20). In addition, the crystal structure of a truncated form of a TtuI protein from *Pyrococcus horikoshii* has been solved (22). Yet, despite these structural studies, the mechanism of enzymes that do not possess an RHD remains unclear because they do not possess a second cysteine, equivalent to *E. coli* Cys456, that would play a similar role as a persulfide transfer site. Furthermore, no other residue has been shown to be involved in catalysis.

Interestingly, TtuI from various archaea, such as *P. furiosus* (PfTtuI) and methanogenic species, have three conserved cysteines located in the catalytic domain (Supplementary Figure S1). These cysteines in TtuI from *Methanococcus maripaludis* (MmTtuI), numbered Cys265, Cys268 and Cys348, have previously been mutated (21). Although the tRNAs from *M. maripaludis* cells expressing the C348A variant possessed only moderate decrease in s^4U level, the decrease was dramatic for cells expressing the C265A or the C268A variant (21). Moreover, in contrast to the wild-type enzyme, none of the three purified mutants was able to transfer sulfur to *in vitro* transcribed *M. jannaschii* $tRNA^{Cys}$, using Na_2S as a sulfur donor, indicating that the three cysteines were required for *in vitro* s^4U-tRNA formation (21). Subsequent electron paramagnetic resonance (EPR) and Mössbauer spectroscopic studies have indicated the presence of a $[3Fe–4S]^+$ cluster in MmTtuI (8). The cluster, most likely coordinated by the conserved cysteines Cys265, Cys268 and Cys348, was proposed to be competent in catalyzing s^4U formation *in vitro* (8).

Intrigued by the unlikely hypothesis of a $[3Fe–4S]^+$ cluster being catalytically active (23) and inspired by previous investigations from ours and other researchers on other tRNA sulfurases that share the same PP-loop ATP pyrophosphatase catalytic domain with TtuI proteins (24), such as tRNA-5-uridine(54)-C2 sulfur transferase TtuA (25–29) and tRNA-5-uridine(34)-C2 sulfur transferases NcsA (Bimai et al., submitted manuscript) and MnmA (30,31), which have been shown to depend on a [4Fe–4S] cluster for activity, we have revisited the mechanism of MmTtuI. To this goal, we have purified untagged versions of MmTtuI and PfTtuI, and reconstituted their cluster *in vitro* under strict anaerobic conditions. We present here spectroscopic analysis and catalytic activity tests that unambiguously show that a $[4Fe–4S]^{2+}$ cluster can be assembled in MmTtuI and PfTtuI and that it is essential for activity. Moreover, we take advantage of the recently released AlphaFold (32) and RoseTTAFold (33) deep learning algorithms to analyze the structural models of MmTtuI in light of our experimental data.

MATERIALS AND METHODS

Genes cloning

The *mmp1354* gene encoding MmTtuI (NCBI WP_011171298.1) and the *pf1288* gene encoding PfTtuI (NCBI WP_011012432.1) were synthesized by Eurofins with codon optimization for expression in *E. coli* and sub-cloned into the pBG102 plasmid (pET27 derivative) between the BamHI and EcoRI restriction sites to produce a 6His-SUMO-TtuI protein construct, the 6His-SUMO tag of which can be cleaved by the human rhinovirus (HRV) 3C protease.

Overexpression of MmTtuI and PfTtuI

The plasmids containing the gene encoding the TtuI proteins were transformed in *E. coli* BL21(*DE3*) competent cells. One colony was used to inoculate 200 ml of Luria Broth (LB) medium supplemented with kanamycin (50 mg. l^{-1}). 40 ml of this preculture grown overnight at 37°C was used to inoculate 4 liters of LB medium supplemented with the same antibiotic. Cultures were grown at 37°C to an OD_{600} of 1–1.2, and expression was induced by addition of isopropyl-γ-D-thiogalactopyranoside (IPTG) to a final concentration of 0.5 mM. After overnight incubation at 25°C, cells were collected by centrifugation and stored at − 20°C.

Purification of MmTtuI and PfTtuI

Cells were resuspended in 60 ml of 50 mM Tris–HCl pH 7.5, 500 mM NaCl, containing RNase A (2 μg.ml^{-1}), benzonase (100 U, Sigma Aldrich) and lysozyme (0.3 mg.ml^{-1}), and disrupted by sonication. Cells debris were removed by centrifugation at 210 000 g for one hour at 4°C. The supernatants were then loaded on an immobilized metal affinity Ni-NTA column (HisTrap 5 ml, Cytiva) equilibrated in 25 mM HEPES pH 7.5, 500 mM NaCl, and eluted with 500 mM imidazole. The proteins were collected, dialyzed overnight against 5 l of 50 mM Tris–HCl pH 7.5 containing 150 mM NaCl (PfTtuI) or 200 mM NaCl (MmTtuI), in the presence of the HRV 3C protease (25 μg per mg TtuI protein), and centrifugated at 4°C for 10 min. MmTtuI was then concentrated to ∼6 mg.ml^{-1} and loaded at 1 ml.min^{-1} in 25 mM HEPES pH 7.5, 200 mM NaCl, onto a Superdex 75 26/60 gel filtration column (Cytiva) using an ÅKTA system, whereas PfTtuI was loaded at 1 ml.min^{-1} onto a Mono S 5/50 cation exchange column (Cytiva), and eluted with a linear gradient of 0-0.5 M NaCl in 25 mM HEPES pH 7.5 for 20 min. The as-purified proteins were concentrated to 10 mg.ml^{-1} with an Amicon Ultra filter device (30 kDa cutoff, Millipore), frozen in liquid nitrogen and stored at -80°C.

The GST-HRV 3C-protease (a gift from S. Mouilleron) was expressed using pGEX-2T recombinant plasmids. After induction at 25°C with 0.1 mM IPTG for 20 h, the protein was purified using glutathione–Sepharose chromatography.

SEC-MALS

Size exclusion chromatography coupled with multi-angle light scattering (SEC-MALS) experiments were performed using an HPLC-MALS system (Shimadzu) equipped with light scattering detector (mini DAWN TREOS, Wyatt Technology), refractive index detector (Optilab T-rEX, Wyatt Technology) and UV detector (SPD-20A, Shimadzu). As-purified MmTtuI (100 μl at 2 mg.ml^{-1}) was injected on a Superdex 200 Increase 10/300 GL column (Cytiva) equilibrated in 50 mM HEPES pH 7.5, 200 mM NaCl, at a flow rate of 0.5 ml.min^{-1}. Molar masses of proteins were calculated with the ASTRA 6.1 software (Wyatt Technology) using a refractive index increment (dn/dc) value of 0.183 ml.g^{-1}.

[Fe–S] cluster reconstitution and purification of holo-TtuI proteins

The reconstitution of the [4Fe–4S] cluster and purification of holo-TtuI proteins were performed in a glove box containing <0.5 ppm O_2. After incubation of 100 μM as-purified TtuI with 5 mM dithiothreitol for 15 min, a 5-fold molar excess of ferrous ammonium sulfate and L-cysteine as well as 2 μM *E. coli* cysteine desulfurase CsdA were added, and incubation was extended overnight. After centrifugation for 20 min at 12 300 g, holo-TtuI was loaded onto a Superdex 200 Increase 10/300 GL gel filtration column (Cytiva) equilibrated in 25 mM HEPES pH 7.5, 200 mM NaCl, 5 mM DTT. The peak containing holo-TtuI was then concentrated to 10–20 mg.ml^{-1} on a Vivaspin concentrator (30 kDa cutoff).

Quantification methods

The Bradford assay was used to quantify the protein (34). The Fish and Beinert methods were routinely used after cluster reconstitution to quantify iron and sulfide, respectively (35,36).

Preparation of bulk tRNA and *in vitro* transcribed Mm-tRNA$^{Lys}_{UUU}$

Bulk tRNA from Δ*thiI E. coli* cells was purified as reported (37). The *M. maripaludis* tRNA$^{Lys}_{UUU}$ substrate (Mm-tRNA$^{Lys}_{UUU}$) was synthesized *in vitro* by T7-RNA polymerase transcription as described (38). Before use, the tRNA transcript was refolded by heating at 65°C for 15 min, at 45°C for 15 min, then cooling slowly to 4°C.

In vitro enzyme assay

1 or 10 μM holo-TtuI and 15–20 μM *in vitro* transcribed Mm-tRNA$^{Lys}_{UUU}$ or 10 μM bulk tRNA from Δ*thiI E. coli* was incubated at 37°C in 100 μl of 25 mM HEPES pH 7.5, 200 mM NaCl in the presence or absence of 1 mM ATP, 2.5 mM $MgCl_2$ and 1 mM Na_2S under anaerobic conditions for 1 hour. The reaction was stopped by adding 1 μl 3M formic acid loading dye. The sulfurated and unmodified tRNAs were separated on a 12% urea Polyacrylamide gel electrophoresis (PAGE) gel supplemented with 15 μg.ml^{-1} APM ([(*N*-acryloylamino)phenyl] mercuric chloride) (39) then visualized by staining with 0.1% [w/v] toluidine in 40% [v/v] methanol and 1% [v/v] acetic acid.

tRNA digestion and analysis of modified nucleosides

20 μM tRNA was digested overnight in 100 μl of 25 mM HEPES pH 7.5, 200 mM NaCl, 0.1 mM $ZnSO_4$ at 37°C by nuclease P1 (2 units, Sigma) followed by the addition of alkaline phosphatase for 2h at 37°C (2 units, Sigma). HPLC-tandem mass spectrometry analyses were performed with an ExionLC chromatographic system coupled with a QTRAP6500 + mass spectrometer (AB SCIEX INSTRUMENTS) equipped with a Turbo Spray IonDrive source used in the positive ionization mode. HPLC separation was carried out with a 2 × 150 mm, 2.7 μm Poroshell HPH-C18 column (Agilent, France) at 0.4 ml.min^{-1} and 35°C. A linear gradient of 0–15% acetonitrile in 0.1% formic acid over 7 min was used as the mobile phase. Mass spectrometry detection was carried out in the multiple reactions monitoring mode to obtain high sensitivity and specificity. The transitions used to quantify s^4U were 261→129 and 261→112, corresponding to the loss of ribose. Under the HPLC conditions used, s^2U and s^4U are well separated, with s^2U eluting faster (4.3 min) than s^4U (4.6 min). Quantification was performed by external calibration.

Characterization of the [4Fe–4S] cluster by UV-Visible and Mössbauer spectroscopies

UV–visible absorption spectra were recorded in quartz cuvettes (1 cm path length) under anaerobic conditions in a glove box on a XL-100 UVIKON spectrophotometer

equipped with optical fibers. The ^{57}Fe metal used for Fe labeling for Mössbauer spectroscopy was rinsed twice with trichloromethane, then solubilized in the glovebox with 1.5 molar equivalent H_2SO_4 by heating at 60°C for 24 h then 78°C for 1 h, under agitation. After centrifugation to remove undissolved particles, the Fe concentration was determined with a calibration curve and the Fish method (35). For Mössbauer spectroscopy, holo-MmTtuI was prepared as above, with ^{57}Fe ferrous sulfate being used during the cluster reconstitution step. After freezing, the samples were stored in liquid nitrogen. Mössbauer spectra of holo-MmTtuI (0.488 mM in 25 mM HEPES pH 7.5, 200 mM NaCl, 5 mM DTT) were recorded in the constant acceleration mode with a WissEL GmbH conventional spectrometer with a multi-channel analyzer in the time-scale mode. Experiments at 77 K were conducted with an LN_2 bath cryostat (Oxford Instruments). The same type of spectrometer was used in the measurement of high-field, low temperature spectra combined with a helium closed-cycle cryostat equipped with a superconducting magnet (CRYO Industries of America Inc.) operating with the applied field parallel to the γ-rays. Isomer shifts δ are given relative to α-iron at room temperature. After transfer of the data from the multi-channel analyzer to a PC, the public domain program Vinda (40) running on an Excel 2003 platform was used to analyze the data. For the simulation of magnetically split spectra, the spin Hamiltonian formalism (41) was utilized. Otherwise, spectra were analyzed by least-squared fits using Lorentzian line shapes.

3D-structure prediction

The AlphaFold models were calculated with the Google Colab platform and AlphaFold2_advanced option https://colab.research.google.com/github/sokrypton/ColabFold/blob/main/beta/AlphaFold2_advanced.ipynb#scrollTo=ITcPnLkLuDDE that does not use templates (homologous structures), and refined using the Amber-relax option to enhance the accuracy of the side chains geometry. The default mode of sampling options was used: num_models = 5, ptm option, num_ensemble = 1, max_cycles = 3, tol = 0, num_samples = 1. The models were ranked according to their predicted local-distance difference test (pLDDT) confidence values (between 0 and 100, from low to high confidence). For dimer prediction, a 1:1 value was input as the homo-oligomer assembly option. The RoseTTAFold models were calculated using the RoseTTAFold option and providing the amino acid sequence to the server https://robetta.bakerlab.org/submit.php.

RESULTS

Purification and characterization of MmTtuI and PfTtuI

MmTtuI, with a N-terminal 6His-SUMO tag, was purified under aerobic conditions by nickel affinity chromatography. The tag was then removed using the HRV 3C protease and the protein was further purified by size-exclusion chromatography (Supplementary Figure S3A and B). SEC-MALS analysis of as-purified MmTtuI indicated that it is a dimer in solution (measured molar mass of 89 ± 0.6 kDa; theoretical molar mass of one monomer: 43.7 kDa) (Supplementary Figure S3C). Careful examination of the UV-visible spectrum of the as-purified MmTtuI protein showed very weak absorption bands, at 320 and 400 nm, characteristic for an [Fe-S] cluster (Figure 1A). This was consistent with the presence of very small amounts of iron and sulfur, 0.03 ± 0.2 mol Fe and 0.05 ± 0.2 mol S per monomer, as quantified using the Beinert and Fish methods (35,36). PfTtuI was also purified under aerobic conditions with a N-terminal 6His-SUMO tag (Supplementary Figure S4A), as described for MmTtuI. In that case again, the UV–visible spectrum of the as-purified PfTtuI protein displayed only very weak absorption bands at 320 and 400 nm, indicating a very low amount of [Fe–S] cluster (Supplementary Figure S4B).

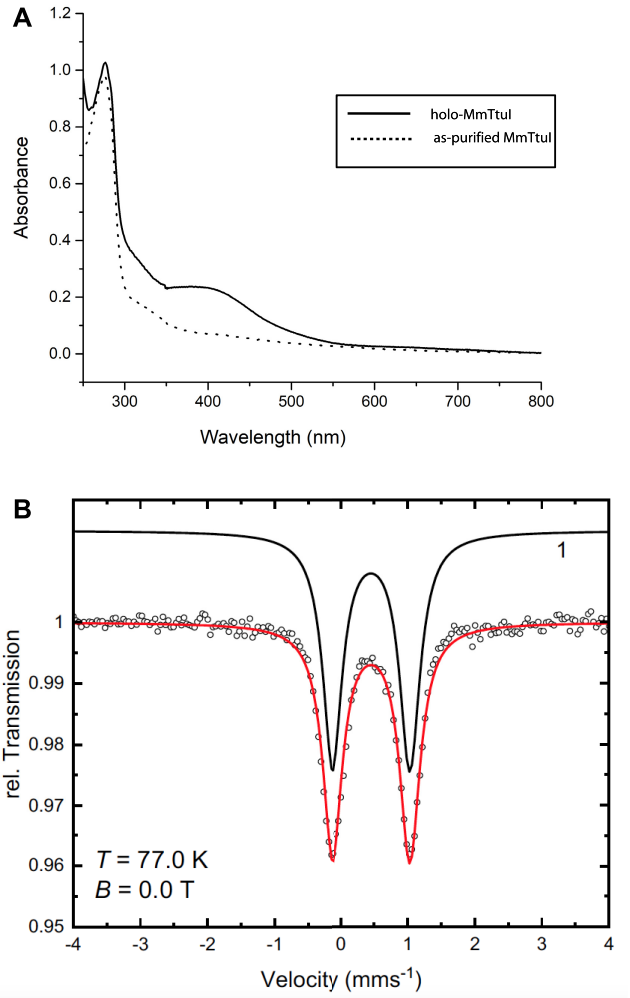

Figure 1. Spectroscopic characterization of MmTtuI. (**A**) UV–visible spectrum of 20 μM as-purified MmTtuI (dotted line) and holo-MmTtuI (solid line) in 25 mM HEPES pH 7.5, 200 mM NaCl. (**B**) Mössbauer spectrum at 77 K and B_{ext} = 0 T of holo-MmTtuI (488 μM) after reconstitution of the cluster with ^{57}Fe. The red solid line is a simulation with the parameters given in Supplementary Table S1.

A [4Fe–4S] cluster can be assembled in MmTtuI anf PfTtuI

A cluster was reconstituted anaerobically by treating the apo-proteins with a 5-molar excess of ferrous iron in the presence of L-cysteine, cysteine desulfurase CsdA and dithiothreitol (DTT) in a glove box containing <0.5 ppm O_2. The protein was then purified on a Superdex 200 gel filtration column (Supplementary Figures S3B, D and S4C, D), also under anaerobic conditions, leading to a homogenous brownish protein, containing an [Fe–S] cluster that was subsequently called holo-TtuI. Quantification of the protein-bound iron and sulfur content gave 3.0 ± 0.2 Fe and 3.1 ± 0.2 S, and 3.2 ± 0.2 Fe and 3.0 ± 0.2 S per monomer of holo-MmTtuI and holo-PfTtuI, respectively, consistent with the presence of one [Fe-S] cluster per monomer. Holo-MmTtuI was obtained as a homogeneous protein in high quantity, whereas much lower amounts of holo-PfTtuI could be obtained since the protein had the tendency to aggregate.

The UV-visible spectra of purified holo-TtuI proteins displayed a broad absorption band at around 400 nm that is characteristic for the presence of a [4Fe–4S] cluster (Figure 1A and Supplementary Figure S4B). From the UV-visible spectrum and Fe/S quantification, a [2Fe–2S] cluster could be excluded. Furthermore, the EPR spectrum of holo-MmTtuI after cluster reconstitution did not show any signal, thus excluding the presence of an EPR active $S = 1/2$ $[3Fe–4S]^{+}$ species. This result is thus consistent with a $S = 0$ $[4Fe–4S]^{2+}$ cluster. The cluster could not be reduced with an excess of dithionite (up to 5 mM, Supplementary Figure S3E), even in the presence of methyl viologen as a redox mediator, or with sodium cyanoborohydride (10 mM), indicating a very low redox potential or inaccessibility of the cluster. To further characterize the chemical state of the cluster by Mössbauer spectroscopy, we used holo-MmTtuI, which could be obtained in high quantity (350 µl at 488 µM), in contrast to holo-PfTtuI. Mössbauer spectroscopy of holo-MmTtuI provides a further confirmation for the presence of a diamagnetic $[4Fe–4S]^{2+}$ cluster (Figure 1B). The Mössbauer spectrum of TtuI obtained at $T = 77$ K shows only one component, exhibiting a doublet with an isomer shift of $\delta = 0.45$ mms^{-1} and a quadrupole splitting of $\Delta E_Q = 1.19$ mms^{-1}. The observed $\delta = 0.45$ mms^{-1} is typical for mixed valence Fe(II)Fe(III) pairs with a delocalized electron occurring in diamagnetic $[4Fe–4S]^{2+}$ clusters. In fact, a Mössbauer spectrum recorded at $T = 4.2$ K and an external field of $B_{ext} = 5.0$ T confirms the presence of a diamagnetic $[4Fe–4S]^{2+}$ cluster and could be simulated using the spin Hamiltonian formalism (41) ($S = 0$, $\delta = 0.45$ mms^{-1}, $\Delta E_Q = 1.19$ mms^{-1}, $\Gamma = 0.49$ mms^{-1}, $\eta = 0.7$) (Supplementary Figure S5 and Table S1) (42). The Mössbauer spectroscopy analysis confirmed the absence of other clusters such as $[2Fe–2S]^{2+}$ and $[3Fe–4S]^{+}$ clusters.

The [4Fe–4S] cluster is needed for the U8-tRNA sulfuration activity

In order to use control samples of MmTtuI and PfTtuI devoid of any Fe and S atoms for the activity assays, the as-purified proteins were treated with dithionite and EDTA and then filtrated, as described (25), to remove any trace

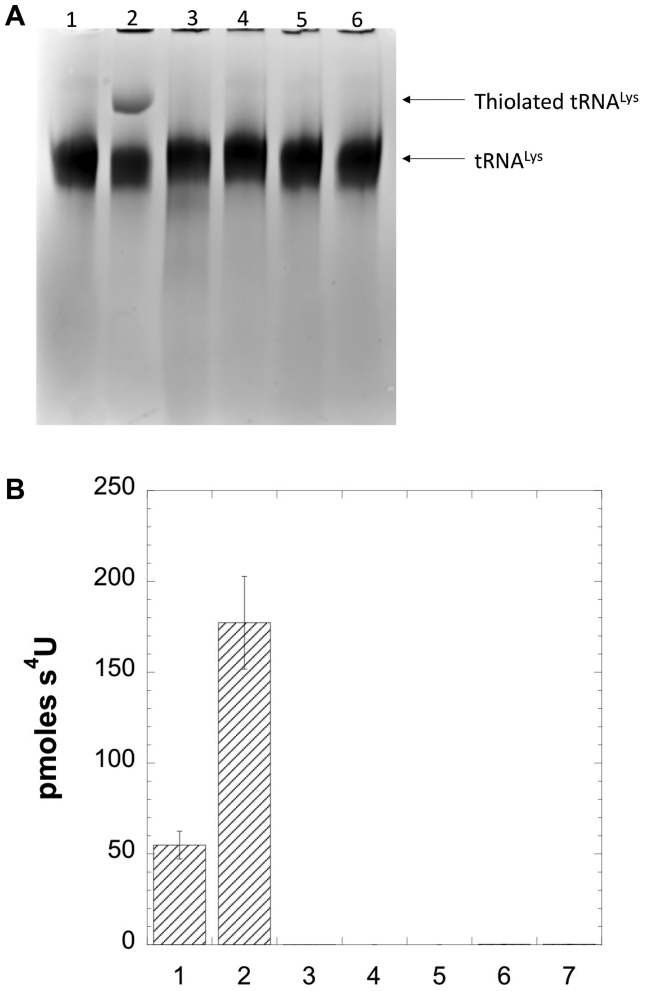

Figure 2. *In vitro* tRNA sulfuration activity tests of MmTtuI under anaerobic conditions. (**A**) The formation of thiolated tRNA was monitored on an APM-retardation gel. 10 µM holo-MmTtuI was incubated with $tRNA^{Lys}_{UUU}$, $MgCl_2$, Na_2S and ATP for 1 h (**2**). Control reactions: $tRNA^{Lys}_{UUU}$ alone (**1**), no Na_2S (**3**), no ATP (**4**), no $MgCl_2$ (**5**), apo-MmTtuI (10 µM) instead of holo-MmTtuI (**6**). (**B**) Quantification of s^4U tRNA sulfuration activity by HPLC-MS/MS. The formation of the s^4U product was monitored by HPLC-coupled MS/MS after tRNA digestion and quantified using a s^4U standard. The data shown are the mean values based on three different experiments. holo-MmTtuI (1 µM (**1**) or 10 µM (**2**)) was incubated with $tRNA^{Lys}_{UUU}$, $MgCl_2$, Na_2S and ATP. Control reactions: no Na_2S (**3**), no ATP (**4**) or no $MgCl_2$ (**5**), apo-MmTtuI (1 µM (**6**) or 10 µM (**7**)) instead of holo-MmTtuI.

of inorganic contaminants and yield the so-called apo-proteins. The sulfuration activity of either apo- or holo-TtuI proteins was tested using *in vitro* transcribed *M. maripaludis* $tRNA^{Lys}_{UUU}$ or bulk tRNA from the *E. coli* Δ*thiI* strain as a substrate, in the presence of inorganic sulfide as the sulfur donor, ATP and Mg^{2+} under strict anaerobic conditions. After 1 hour incubation, tRNA sulfuration was monitored using a denaturing urea PAGE gel containing APM (39), which specifically retards migration of sulfur-containing molecules and thus separates sulfurated tRNAs from unmodified tRNAs (Figure 2A and Supplementary Figure S4E). A band corresponding to the sulfurated tRNA was observed on the gel only when holo-

MmTtuI was incubated with tRNA and all other components (Na_2S, ATP, Mg^{2+}) of the assay mixture. Moreover, no such band was obtained when the apo-TtuI proteins were used instead of the holo-TtuI proteins. These experiments thus showed that the cluster, inorganic sulfide, ATP and Mg^{2+} were all required for the tRNA sulfuration activity of MmTtuI. For the identification of the modified nucleoside (s^4U) and quantification, the tRNA products after MmTtuI treatment were digested into nucleosides that were analyzed by HPLC MS/MS using s^4U as a standard (Supplementary Figure S6). Whereas the controls containing no enzyme, no ATP, no Na_2S, no Mg^{2+} or apo-MmTtuI showed no formation of modified nucleosides, the presence of s^4U was observed exclusively when holo-MmTtuI was incubated in the presence of all reactants, with the amount of s^4U increasing with increased concentration of holo-MmTtuI (Figure 2B). Altogether, our activity tests clearly showed that the [4Fe–4S] cluster is necessary for MmTtuI to function as a U8-tRNA sulfurase.

In the AlphaFold and RoseTTAFold models of MmTtuI, Cys265, Cys268 and Cys348 are correctly positioned to bind a [4Fe–4S] cluster

We obtained small crystals of holo-MmTtuI but their size was not sufficient to yield exploitable crystallographic data. Therefore, in the absence of a crystal structure of MmTtuI, we calculated 3D models using the AlphaFold (32) and RoseTTAFold (33) algorithms, which have recently been shown to predict very precisely not only the fold of a protein from its amino acid sequence, but also the amino acid side chains position when the backbone position is accurate. The models of the MmTtuI monomer are predicted with a high confidence (pLDDT of 95.6 and confidence value of 0.86, for the AlphaFold and RoseTTAFold models, respectively) and exhibit an elongated fold, organized into two main structural domains: the N-terminal domain and the C-terminal catalytic domain that contains the ATP binding site (Figure 3A). The AlphaFold and RoseTTAFold models of the MmTtuI monomer are highly similar, with a root mean square deviation (rmsd) of 1.12 Å over 336 aligned Cαs, except for the last C-terminal helix (residues 376–382) that shows completely different orientations in the two models. The three conserved cysteines are located near each other in both AlphaFold and RoseTTaFold models (Figure 3B). However, while Cys265 and Cys268 from one model overlap well with the same residues in the second model, the positions of the sulfur atom of Cys348, which belongs to a flexible loop, are 3.7 Å apart in the two models. Such a modeling uncertainty was previously noted for other cysteines from flexible loops that coordinate a [4Fe–4S] cluster in other [Fe-S]-binding proteins (43). The positioning of Cys265, Cys268 and Cys348, in the heart of the active site and close to each other, together with previously reported site-directed mutagenesis experiments that showed the importance of these cysteines for s^4U formation (21), is highly in favor with these three cysteines being the ligands of the [4Fe–4S] cluster in holo-MmTtuI.

Moreover, the binding mode of the [4Fe–4S] cluster to MmTtuI can be inferred from the superposition of the MmTtuI models with the crystal structure of the [4Fe–4S]-dependent U54-tRNA sulfurtransferase TtuA from *Pyrococcus horikoshii* (holo-PhTtuA) (25). Indeed, despite the low sequence identity (14.8%) between MmTtuI and PhTtuA, their catalytic domains are structurally similar (rmsd = 3.9 Å, *Z*-score of 12.3 for 157 aligned Cαs, as calculated with DALI) (44), reflecting their belonging to the N-type ATPase family. The superposition of the catalytic domains of the two enzymes indeed places the [4Fe–4S] cluster of holo-PhTtuA close enough to the three cysteines of MmTtuI to validate a [4Fe–4S] cluster at this position in holo-MmTtuI (Figure 3C). Indeed, the sulfur atoms of Cys265, Cys268 and Cys348 of MmTtuI are located 3.5–6.4 Å, 3.4–3.7 Å and 1.8–4.0 Å away from the iron atoms of the [4Fe–4S] cluster in the superimposed holo-PhTtuA structure, respectively, indicating that only small conformational changes in the active site loops and cysteine residues of MmTtuI are needed to accommodate the correct geometry required to bind the [4Fe–4S] cluster.

Comparison of the MmTtuI models with the BaTtuI and TmTtuI crystal structures

The crystal structures of two TtuI enzymes that do not possess the C-terminal RHD have been solved previously: BaTtuI in complex with AMP (19) and TmTtuI in complex with a mini-RNA, in the presence or absence of ATP (20). It should be noted that the TmTtuI/mini-RNA/ATP complex represents an initial inactive state, the U8 target uridine being not flipped out and thus not oriented towards the enzyme active site. Nevertheless, to validate the MmTtuI models, it is interesting to compare them to the BaTtuI and TmTtuI crystal structures. Both the MmTtuI dimer, which was predicted with a high confidence with AlphaFold (pLDDT of 94.1), and the MmTtuI monomer modeled by AlphaFold or RoseTTaFold can be superimposed closely to the dimer or monomer of TmTtuI and BaTtuI (Figure 3D and Supplementary Figure S7A), in agreement with the high amino acid sequence identity (30.5% between MmTtuI and TmTtuI, and 30.8% between MmTtuI and BaTtuI; Supplementary Figure S1). In addition, the superposition of the active sites of the MmTtuI models with those of the two molecules of the TmTtuI/ATP crystal structure (Figure 3E and F) and that of the BaTtuI/AMP crystal structure (Supplementary Figure S7B), shows that the three cysteines of MmTtuI are located near the AMP/ATP cofactors found in the TmTtuI and BaTtuI structures, suggesting a similar ATP binding mode in MmTtuI. Mutation of Cys344 to serine in TmTtuI has been shown to lead to a complete loss of activity, indicating that Cys344 is a catalytically essential residue (20). In the TmTtuI crystal structure, Cys344 belongs to a long flexible loop that exhibits two different conformations in the two molecules in the asymmetric unit (Figure 3E and F), whereas Cys344 and Cys345 of BaTtuI, also belonging to a flexible loop, were not observed in the electron density of the BaTtuI crystal. Interestingly, the superposed structures show that, whereas Cys344 in molecule A of TmTtuI is quite distant from the cysteines of MmTtuI, in molecule B it occupies a position very close to that of Cys348 in the MmTtuI models (the sulfur atom of Cys344 being distant of 1.8 and 2.1 Å of the sulfur atoms of Cys348 in the AlphaFold and RoseTTAFold models, respectively).

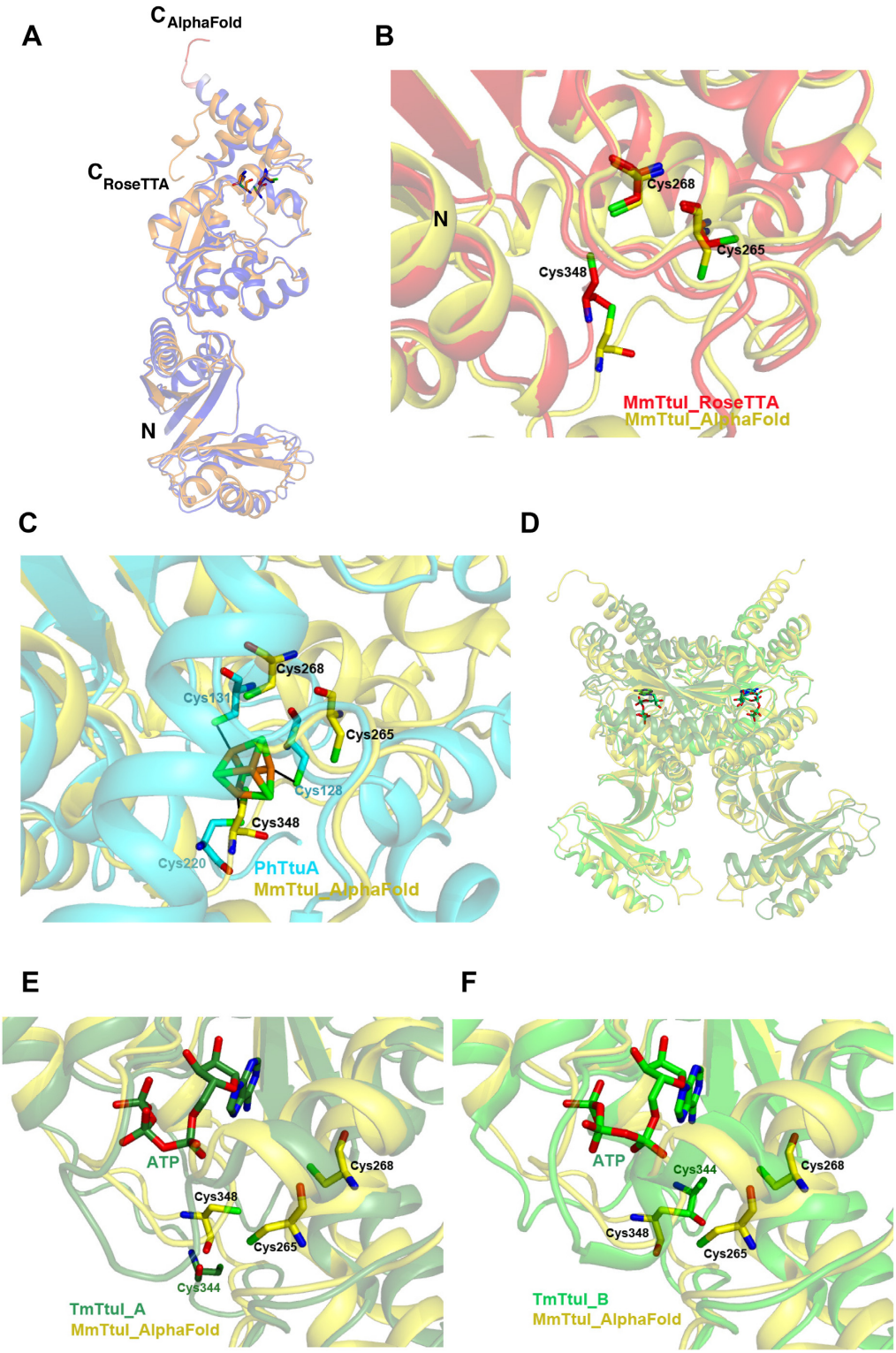

Figure 3. Best models of MmTtuI. (**A**) Superposition of the AlphaFold model, colored according to the pLDDT values, from red (pLDDT value of 37.0) to blue (pLDDT value of 98.8) and RoseTTAFold (in orange) model of the monomer of MmTtuI. (**B**) Superposition of the conserved cysteines of MmTtuI in the AlphaFold model (in yellow) and RoseTTAFold model (in red). The pLDDT values of Cys265, Cys268 and Cys348 in the AlphaFold model are 95.8, 95.9 and 89.4, respectively. (**C**) Superposition of the active sites of the MmTtuI AlphaFold model and holo-PhTtuA crystal structure (PDB code 5MKP, in cyan). Holo-PhTtuA was superimposed onto the MmTtuI model with the *SUPER* option in PYMOL, with an rmsd of 3.4 Å for 98 aligned Cα atoms. The cluster in holo-PhTtuA is shown in stick representation. (**D**) Superposition of the dimer of MmTtuI calculated with AlphaFold with that of the crystal structure of TmTtuI (in green and forest green for each monomer). ATP bound to TmTtuI is shown in stick representation. (**E**, **F**) Superposition of the active sites of the MmTtuI AlphaFold model and TmTtuI crystal structure (**E**: molecule A of TmTtuI; **F**, molecule B of TmTtuI). The MmTtuI model is superimposed on molecules A and B of the TmTtuI crystal structures with an rmsd of 1.37 Å for 281 aligned Cα atoms and an rmsd of 1.48 Å for 285 aligned Cα atoms, respectively. ATP and Cys344 in the TmTtuI structure are shown in stick representation.

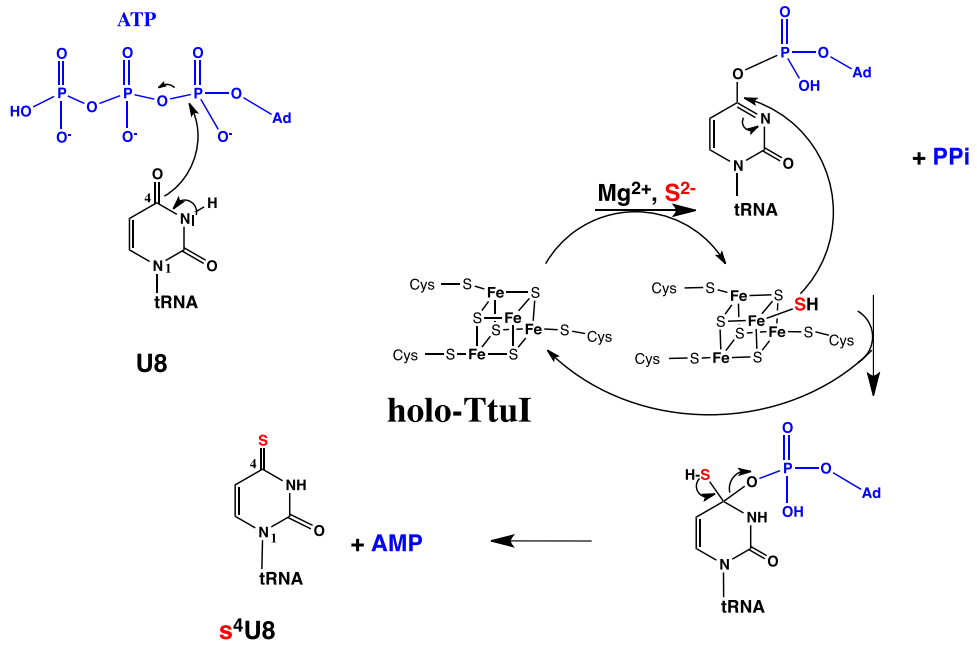

Figure 4. Mechanism proposed for the MmTtuI-catalyzed reaction. Ad stands for 'adenylate'. After adenylation at O4 by ATP and formation of a [4Fe–5S] cluster intermediate, nucleophilic substitution of O-adenosyl monophosphate by the SH group coordinated by the [4Fe–4S] cluster would generate the final s^4U8-tRNA product.

DISCUSSION

We report here that as-purified MmTtuI and PfTtuI can be reconstituted under anaerobic conditions with a [4Fe–4S] cluster, which was shown to be crucial for the U8-tRNA sulfuration activity. The fact that Liu *et al.* previously observed U8-sulfuration activity (although not quantified) of [3Fe–4S]-cluster containing MmTtuI (8) is puzzling given that nonredox [Fe–S]-catalyzed reactions usually depend on a [4Fe–4S] cluster, the active state of the cluster (23), with the [3Fe–4S] species being an oxidation product of the former species (45). One possible explanation could be the presence of a small amount of catalytically active [4Fe–4S] cluster in the preparation, however in too low quantity to be detectable by spectroscopy. Another possibility is that some [4Fe–4S] cluster could form during catalysis, via reductive conversion of the [3Fe–4S] species in the presence of iron traces under the highly reducing conditions in the catalytic assay (8).

The AlphaFold and RoseTTAFold models of MmTtuI show that the three conserved cysteines, Cys265, Cys268 and Cys348, are correctly positioned to bind a [4Fe–4S] cluster. This prediction agrees with Cys265 and Cys268 being crucial for *in vivo* s^4U tRNA sulfurase activity, as shown by their mutation to alanine leading to a dramatic decrease of s^4U levels in tRNAs (21). Yet, the C348A mutant showed only a modest decrease of s^4U, with 62% that of the wild-type level, but this result is not against Cys348 being a cluster ligand, as shown for other [4Fe–4S]-dependent enzymes, for which the mutation of only one coordinating cysteine was not sufficient to completely abolish cluster binding (30). The subsequent prediction from the 3D models is that the [4Fe–4S] cluster in holo-MmTtuI would be bound by these three cysteines only, without the need of a fourth amino acid ligand. Altogether, our experimental data and the 3D models lead us to propose a mechanism for the MmTtuI-catalyzed reaction, based on that of [4Fe–4S]-dependent tRNA-sulfurtransferases such as TtuA (25–29), in which the fourth non-protein bonded Fe atom of the cluster (unique Fe atom) is used to bind and activate the sulfur atom of the donor in the form of a hydrogenosulfide ligand (Figure 4). This would lead to the formation of [4Fe–5S] cluster intermediate, the existence of which was revealed in the case of TtuA and NcsA enzymes by the propensity of the unique Fe atom of the cluster to bind a small molecule (25, PDB code 6SCY), and demonstrated in the case of thiouracil desulfidase TudS (46), which catalyzes a [4Fe–4S]-dependent desulfuration reaction, the inverse reaction to that catalyzed by TtuI enzymes. After activation of the target U8 by adenylation by ATP to form an adenylated intermediate, attack of the hydrogenosulfide bound to the [4Fe–4S] cluster onto the C4 position would result into nucleophilic substitution, release of AMP and formation of the thiouridine product. The activation of the target uridine of TtuI by adenylation of its C4 position by ATP (16) differs from the substrate activation mechanism in nonredox [4Fe–4S]-dependent dehydratases, such as aconitase (47), in which the unique Fe atom of the cluster directly binds the hydroxyl group of the substrate to initiate the dehydration reaction.

CONCLUSION

Our work confirms the existence of a new class of TtuI proteins that operate with a [Fe–S] cluster (8). However, our biochemical and spectroscopic results indicate that the catalytic state of the cluster is a $[4Fe–4S]^{2+}$ and not a

$[3Fe–4S]^{+}$ species, as stated previously (8). Given precedent studies on similar [4Fe–4S]-dependent tRNA sulfurases (25,26,28,30,31), we propose a mechanism for MmTtuI, in which the fourth, nonprotein-bonded iron of the cluster binds and activates a hydrogenosulfide substrate to catalyze the nonredox substitution of an oxygen atom for a sulfur atom (Figure 4). It remains to be seen whether two or three classes of TtuI proteins exist. In addition to proteins like EcTtuI that possess an RHD, in which a catalytic cysteine is thought to receive a sulfur atom and form a persulfide, the sulfur of which is transferred to U8, and those like MmTtuI, which possess a conserved CXXC + C motif and bind a [4Fe–4S] cluster that is used as a cofactor, the enzymes that function neither with an RHD nor a CXXC + C motif need further investigation.

DATA AVAILABILITY

All data are available from the authors upon request. The AlphaFold and RoseTTA models are easily calculated as described. The AlphaFold models of the complexes are accessible via the following links: DOI: http://dx.doi.org/10.13140/RG.2.2.35001.24164, AlphaFold model of the MmTtuI dimer; DOI: http://dx.doi.org/10.13140/RG.2.2.33323.52005, AlphaFold model of the MmTtuI monomer; DOI: http://dx.doi.org/10.13140/RG.2.2.23257.19043, RoseTTAFold model of the MmTtuI monomer.

SUPPLEMENTARY DATA

Supplementary Data are available at NAR Online.

ACKNOWLEDGEMENTS

This work was supported by the French State Program ‘Investissements d’Avenir’ (Grants ‘LABEX DYNAMO’, ANR-11-LABX-0011) and has benefited from the facilities and expertise of the Macromolecular Interaction Platform of I2BC. We thank Nadia Touati and the French EPR CNRS Facility, Infrastructure de Recherche Renard (IR 3443) for preliminary EPR experiments; Ludovic Pecqueur for maintenance of the glove boxes.

FUNDING

French EPR CNRS Facility [IR 3443]; French state Program Labex [ANR-11-LABX-0011]. Funding for open access charge: LABEX DYNAMO [ANR-11-LABX-0011].
Conflict of interest statement. None declared.

REFERENCES

1. Björk,G.R. (1995) Genetic dissection of synthesis and function of modified nucleosides in bacterial transfer RNA. *Prog. Nucleic Acid Res. Mol. Biol.*, **50**, 263–338.
2. Kotera,M., Bayashi,T., Hattori,M., Tokimatsu,T., Goto,S., Mihara,H. and Kanehisa,M. (2010) Comprehensive genomic analysis of sulfur-relay pathway genes. *Genome Inform.*, **24**, 104–115.
3. Favre,A., Michelson,A.M. and Yaniv,M. (1971) Photochemistry of 4-thiouridine in *Escherichia coli* transfer RNA1Val. *J. Mol. Biol.*, **58**, 367–379.
4. Kramer,G.F., Baker,J.C. and Ames,B.N. (1988) Near-UV stress in *Salmonella typhimurium*: 4-thiouridine in tRNA, ppGpp, and ApppGpp as components of an adaptive response. *J. Bacteriol.*, **170**, 2344–2351.
5. Mueller,E.G., Buck,C.J., Palenchar,P.M., Barnhart,L.E. and Paulson,J.L. (1998) Identification of a gene involved in the generation of 4-thiouridine in tRNA. *Nucleic Acids Res.*, **26**, 2606–2610.
6. Bender,R.A. (2011) The danger of annotation by analogy: most “thiI” genes play no role in thiamine biosynthesis. *J. Bacteriol.*, **193**, 4574–4575.
7. Rajakovich,L.J., Tomlinson,J. and Dos Santos,P.C. (2012) Functional analysis of *Bacillus subtilis* genes involved in the biosynthesis of 4-Thiouridine in tRNA. *J. Bacteriol.*, **194**, 4933–4940.
8. Liu,Y., Vinyard,D.J., Reesbeck,M.E., Suzuki,T., Manakongtreecheep,K., Holland,P.L., Brudvig,G.W. and Söll,D. (2016) A [3Fe-4S] cluster is required for thiolation in archaea and eukaryotes. *Proc. Natl. Acad. Sci. U.S.A.*, **113**, 12703–12708.
9. Martinez-Gomez,N.C., Palmer,L.D., Vivas,E., Roach,P.L. and Downs,D.M. (2011) The rhodanese domain of ThiI is both necessary and sufficient for synthesis of the thiazole moiety of thiamine in *Salmonella enterica*. *J. Bacteriol.*, **193**, 4582–4587.
10. Tomikawa,C., Ohira,T., Inoue,Y., Kawamura,T., Yamagishi,A., Suzuki,T. and Hori,H. (2013) Distinct tRNA modifications in the thermo-acidophilic archaeon, *Thermoplasma acidophilum*. *FEBS Lett.*, **587**, 3575–3580.
11. Kambampati,R. and Lauhon,C.T. (2000) Evidence for the transfer of sulfane sulfur from IscS to ThiI during the in vitro biosynthesis of 4-thiouridine in *Escherichia coli* tRNA. *J. Biol. Chem.*, **275**, 10727–10730.
12. Lauhon,C.T. and Kambampati,R. (2000) The *iscS* gene in *Escherichiacoli* is required for the biosynthesis of 4-thiouridine, thiamin, and NAD. *J. Biol. Chem.*, **275**, 20096–20103.
13. Fislage,M., Roovers,M., Tuszynska,I., Bujnicki,J.M., Droogmans,L. and Versees,W. (2012) Crystal structures of the tRNA:m2G6 methyltransferase Trm14/TrmN from two domains of life. *Nucleic Acids Res.*, **40**, 5149–5161.
14. Gabant,G., Auxilien,S., Tuszynska,I., Locard,M., Gajda,M.J., Chaussinand,G., Fernandez,B., Dedieu,A., Grosjean,H., Golinelli-Pimpaneau,B. *et al.* (2006) THUMP from archeal tRNA:m22G methyltransferase, a genuine autonomously folding domain. *Nucleic Acids Res.*, **34**, 2483–2494.
15. Randau,L., Stanley,B.J., Kohlway,A., Mechta,S., Xiong,Y. and Soll,D. (2009) A cytidine deaminase edits C to U in transfer RNAs in archaea. *Science*, **324**, 657–659.
16. You,D., Xu,T., Yao,F., Zhou,X. and Deng,Z. (2008) Direct evidence that ThiI is an ATP pyrophosphatase for the adenylation of uridine in 4-thiouridine biosynthesis. *Chembiochem.*, **9**, 1879–1882.
17. Mueller,E.G., Palenchar,P.M. and Buck,C.J. (2001) The role of the cysteine residues of ThiI in the generation of 4-thiouridine in tRNA. *J. Biol. Chem.*, **276**, 33588–33595.
18. Wright,C.M., Palenchar,P.M. and Mueller,E.G. (2002) A paradigm for biological sulfur transfers via persulfide groups: a persulfide-disulfide-thiol cycle in 4-thiouridine biosynthesis. *Chem. Commun.*, **22** , 2708–2709.
19. Waterman,D.G., Ortiz-Lombardia,M., Fogg,M.J., Koonin,E.V. and Antson,A.A. (2006) Crystal structure of *Bacillus anthracis* ThiI, a tRNA-modifying enzyme containing the predicted RNA-binding THUMP domain. *J. Mol. Biol.*, **356**, 97–110.
20. Neumann,P., Lakomek,K., Naumann,P.T., Erwin,W.M., Lauhon,C.T. and Ficner,R. (2014) Crystal structure of a 4-thiouridine synthetase-RNA complex reveals specificity of tRNA U8 modification. *Nucleic Acids Res.*, **42**, 6673–6685.
21. Liu,Y., Zhu,X., Nakamura,A., Orlando,R., Söll,D. and Whitman,W.B. (2012) Biosynthesis of 4-thiouridine in tRNA in the methanogenic archaeon *Methanococcus maripaludis*. *J. Biol. Chem.*, **287**, 36683–36692.
22. Sugahara,M., Murai,S. and Kunishima,N. (2007) Purification, crystallization and preliminary crystallographic analysis of the putative thiamine-biosynthesis protein PH1313 from P*yrococcus horikoshii* OT3. *Acta Crystallogr. Sect. F. Struct. Biol. Cryst. Commun.*, **63**, 56–58.
23. Flint,D.H. and Allen,R.M. (1996) Iron-sulfur proteins with nonredox functions. *Chem. Rev.*, **96**, 2315–2334.

24. Bimai,O., Arragain,S. and Golinelli-Pimpaneau,B. (2020) Structure-based mechanistic insights into catalysis by tRNA thiolation enzymes. *Curr. Opin. Struct. Biol.*, **65**, 69–78.
25. Arragain,S., Bimai,O., Legrand,P., Caillat,S., Ravanat,J.L., Touati,N., Binet,L., Atta,M., Fontecave,M. and Golinelli-Pimpaneau,B. (2017) Nonredox thiolation in tRNA occurring via sulfur activation by a [4Fe–4S] cluster. *Proc. Natl. Acad. Sci. U.S.A.*, **114**, 7355–7360.
26. Chen,M., Asai,S.I., Narai,S., Nambu,S., Omura,N., Sakaguchi,Y., Suzuki,T., Ikeda-Saito,M., Watanabe,K., Yao,M. *et al.* (2017) Biochemical and structural characterization of oxygen-sensitive 2-thiouridine synthesis catalyzed by an iron-sulfur protein TtuA. *Proc. Natl. Acad. Sci. U.S.A.*, **114**, 4954–4959.
27. Chen,M. and Tanaka,Y. (2019) In: Wiley,S.E. (ed). *Encyclopedia of Inorganic and Bioinorganic Chemistry*. Wiley, Chichester, UK.
28. Chen,M., Ishizaka,M., Narai,S., Horitani,M., Shigi,N., Yao,M. and Tanaka,Y. (2020) The [4Fe–4S] cluster of sulfurtransferase TtuA desulfurizes TtuB during tRNA modification in *Thermus thermophilus*. *Commun. Biol.*, **3**, 168.
29. Zhou,J., Bimai,O., Arragain,S., Pecqueur,L. and Golinelli-Pimpaneau,B. (2022) In: Wiley,S.E. (ed). *Encyclopedia of Inorganic and Bioinorganic Chemistry*. Wiley, Chichester, UK.
30. Shigi,N., Horitani,M., Miyauchi,K., Suzuki,T. and Kuroki,M. (2020) An ancient type of MnmA protein is an iron-sulfur cluster-dependent sulfurtransferase for tRNA anticodons. *RNA*, **26**, 240–250.
31. Zhou,J., Lénon,M., Touati,N., Ravanat,J.-L., Velours,C., Fontecave,M., Barras,F. and Golinelli-Pimpaneau,B. (2021) Iron sulfur biology invades tRNA modification: the case of U34 sulfuration. *Nucleic Acids Res.*, **49**, 3997–4007.
32. Jumper,J., Evans,R., Pritzel,A., Green,T., Figurnov,M., Ronneberger,O., Tunyasuvunakool,K., Bates,R., Žídek,A., Potapenko,A. *et al.* (2021) Highly accurate protein structure prediction with alphafold. *Nature*, **596**, 583–589.
33. Baek,M., DiMaio,F., Anishchenko,I., Dauparas,J., Ovchinnikov,S., Lee,G.R., Wang,J., Cong,Q., Kinch,L.N., Schaeffer,R.D. *et al.* (2021) Accurate prediction of protein structures and interactions using a three-track neural network. *Science*, **373**, 871–876.
34. Bradford,M.M. (1976) A rapid and sensitive method for the quantitation of microgram quantities of protein utilizing the principle of protein-dye binding. *Anal. Biochem.*, **72**, 248–254.
35. Fish,W.W. (1988) Rapid colorimetric micromethod for the quantitation of complexed iron in biological samples. *Methods Enzymol.*, **158**, 357–364.
36. Beinert,H. (1983) Semi-micro methods for analysis of labile sulfide and of labile sulfide plus sulfane sulfur in unusually stable iron-sulfur proteins. *Anal. Biochem.*, **131**, 373–378.
37. Buck,M., Connick,M. and Ames,B.N. (1983) Complete analysis of tRNA-modified nucleosides by high performance liquid chromatography: the 29 modified nucleosides of *Salmonella typhimurium* and *Escherichia coli*. *Anal. Biochem.*, **129**, 1–13.
38. Milligan,J.F., Groebe,D.R., Witherell,G.W. and Uhlenbeck,O.C. (1987) Oligoribonucleotide synthesis using T7 RNA polymerase and synthetic DNA templates. *Nucleic Acids Res.*, **15**, 8783–8798.
39. Biondi,E. and Burke,D.H. (2012) Separating and analyzing sulfur-containing RNAs with organomercury gels. *Methods Mol. Biol.*, **883**, 111–120.
40. Gunnlaugsson,H.P. (2016) Spreadsheet based analysis of Mössbauer spectra. *Hyperfine Interact*, **237**, 13–18.
41. Gütlich,P., Bill,E. and Trautwein,A.X. (2011) In: *Mössbauer Spectroscopy and Transition Metal Chemistry*. Springer Berlin Heidelberg, Berlin, Heidelberg.
42. Pandelia,M.E., Lanz,N.D., Booker,S.J. and Krebs,C. (2015) Mössbauer spectroscopy of Fe/S proteins. *Biochim. Biophys. Acta.*, **1853**, 1395–1405.
43. Golinelli-Pimpaneau,B. (2022) Prediction of the iron–sulfur binding sites in proteins using the highly accurate three-dimensional models calculated by AlphaFold and RoseTTAFold. *Inorganics*, **10**, 2.
44. Holm,L. (2020) DALI and the persistence of protein shape. *Protein Sci.*, **29**, 128–140.
45. Crack,J.C., Jervis,A.J., Gaskell,A.A., White,G.F., Green,J., Thomson,A.J. and Le Brun,N.E. (2008) Signal perception by FNR: the role of the iron-sulfur cluster. *Biochem. Soc. Trans.*, **36**, 1144–1148.
46. Zhou,J., Pecqueur,L., Aučynaitė,A., Fuchs,J., Rutkienė,R., Vaitekūnas,J., Meškys,R., Boll,M., Fontecave,M., Urbonavičius,J. *et al.* (2021) Structural evidence for a [4Fe-5S] intermediate in the non-redox desulfuration of thiouracil. *Angew. Chem. Int. Ed. Engl.*, **60**, 424–431.
47. Beinert,H., Kennedy,M.C. and Stout,C.D. (1996) Aconitase as iron-sulfur protein, enzyme, and iron-regulatory protein. *Chem. Rev.*, **96**, 2335–2374.